Design and development of a snapshot imaging spectropolarimeter

Derek S. Sabatke, Ann M. Locke, Eustace L. Dereniak,
John P. Garcia, Christopher P. Tebow
University of Arizona, Tucson, AZ 85721

David Sass
US Army TACOM, Warren, MI 48397

ABSTRACT

A snapshot imaging spectropolarimeter is under development. The instrument operates through the synthesis of the techniques of computed tomography imaging spectrometry (CTIS) and channeled spectropolarimetry. CTIS is a technique of imaging spectrometry in which an image of a scene is captured through a computer-generated holographic disperser. Spatially resolved spectra are reconstructed from the diffracted orders in post-processing. Channeled spectropolarimetry is a method of encoding the four components of a spectrally varying Stokes vector into a single irradiance spectrum. The combination of the two techniques provides the basis of an imaging spectropolarimeter capable of acquiring a complete data set in a single focal plane array integration time with no moving parts.

Our description of the instrument includes a review of the basic principles of both techniques. The diffraction orders generated by the CTIS disperser amount to projections through the scene's object cube, which provide an analogy to the medical imaging technique of computed tomography. Channeled spectropolarimetry is analogous to sideband modulation (as may be used in radio communication). Thick (high order) retarders and a polarizer are employed to introduce modulation. This viewpoint provides a starting point for the formulation of system requirements and reconstruction techniques. The requisite spectral resolution of the embedded spectrometer and selection of carrier frequencies by design of the retarders are addressed. We also discuss the design of a prototype snapshot imager for the visible spectrum and describe a non-imaging spectropolarimeter for the development of calibration and data reduction techniques.

1 INTRODUCTION

Imaging spectrometry and polarimetry are promising techniques for the detection and identification of manmade objects in natural backgrounds. Spectrometry enables detailed comparison of target and background spectra. Polarimetry allows the observer to capitalize on the fact that light emitted from and reflected by smooth surfaces tends to acquire a polarized component.[1] Polarization information then has the potential to highlight manmade objects despite spectral camouflage. We report on development of an imaging instrument which integrates both spectrometry and polarimetry functions. The instrument will be capable of characterizing the state of polarization of radiation from each pixel of a target scene by measuring all four components of the Stokes vector as a function of wavelength.

The data acquired can be interpreted as an image of a four-dimensional volume, since a measure of radiance is obtained for four independent variables or indices: two spatial variables (x, y), wavenumber (σ), and the Stokes vector index (j). It should be noted however that the Stokes vector index has only four possible values (the integers from 0 to 3), whereas the x, y, and σ dimensions will each be segmented into a greater number of intervals. We refer to this four-dimensional volume as the spectropolarimetric hypercube. For example, our goal for a proof-of-principle

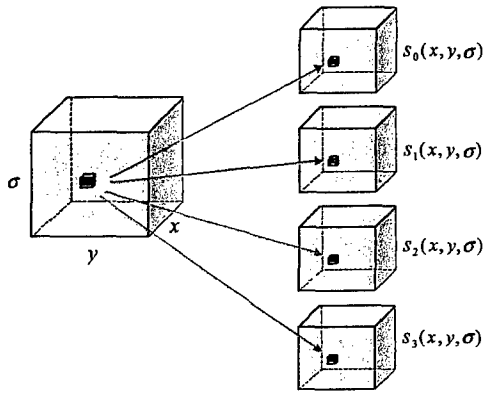

Figure 1: An illustration of the four-dimensional (x, y, σ, j) nature of the data acquired by an imaging spectropolarimeter.

system for the visible spectrum is to obtain on the order of 50×50 pixel spatial resolution with 16 wavelength bands in the spectral image for each Stokes component. Figure 1 illustrates the concept of the four-dimensional hypercube.

Conventional spectrometers and polarimeters are generally unable to image all of the dimensions of the hypercube at once. They are inherently sensitive to a one-, two-, or three-dimensional subset of the volume, and must scan out the remaining dimensions in some manner. For example, a camera with a narrow-band filter could be used to obtain a single x,y slice through the hypercube. In this slice x and y vary while σ is fixed at the wavenumber passed by the filter and j is held at zero. The entire four dimensions could be swept out by swapping in filters with different transmission wavelengths and sets of polarizers and retarders, using two independent filter wheels in front of the camera. Similar examples can be made for other systems, such as slit spectrometers and whisk broom scanners (see Figure 2).

Two drawbacks of systems which require scanning are immediately apparent. First, moving parts (such as rotating filter wheels and dithering mirrors) are generally employed, and these are undesirable from the standpoint of reliability. Second, a relatively long time is required for the capture of a complete data set, since multiple exposures are made sequentially in time. Changes in the target scene during scanning manifest themselves as artifacts in the results. Scanning systems thus have limited ability to acquire data on rapidly changing scenes, such as moving targets or targets viewed from moving platforms. A brute force method for avoiding scanning is to use several separate systems viewing the same scene in parallel, possibly with beam splitters to direct light to each. Such systems tend to be expensive, however, since multiple focal plane arrays (FPAs) and a considerable investment in optics are generally involved. Furthermore, registration of the images from the separate systems is problematic.

The system under development promises to circumvent these difficulties via snapshot capability. It will capture data with coverage of the entire hypercube in a single integration time with a single FPA.

1.1 Channeled spectropolarimetry

The instrument will operate through the fusion of two techniques: channeled spectropolarimetry[2–4] and computed tomography imaging spectrometry.[5] Accordingly, it is referred to hereafter as a computed tomography imaging channeled spectropolarimeter (CTICS). Figure 3 illustrates the principle of operation of a channeled spectropolarimeter. The radiation under analysis is passed through two thick (high order) retarders and a polarizer, and the spectrum of the exiting light is recorded by a spectrometer. The fast axis of the first retarder is aligned with the transmission axis of the polarizer, and the second retarder is oriented with its fast axis at 45° to the polarizer's axis.

The recorded spectrum is a linear superposition of the Stokes component spectra of the incident light, in which the coefficients are sinusoidal terms depending on the retardances of the retarders. Since each retardance is nominally proportional to wavenumber σ, the Stokes component spectra are modulated. With proper choice of modulation

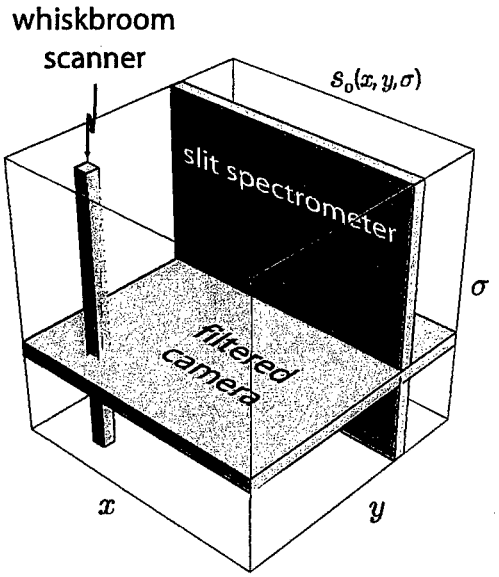

Figure 2: The lower-dimensional volumes which various spectrometer types are capable of imaging without scanning. Such spectrometers could be used with scanning to obtain spectral and spatial data on the s_0 polarization component, with additional measures (such as swapping of polarizers and retarders) necessary to obtain complete polarimetric data.

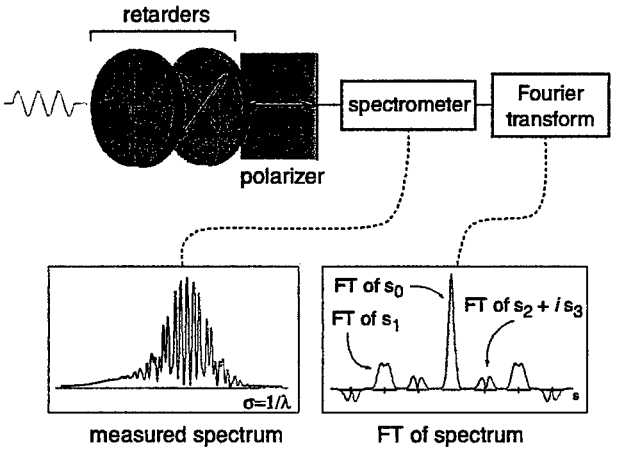

Figure 3: The channeled spectropolarimeter (after Oka and Kato[2]). The complex spectrum recorded at the output of the polarization optics is formed by a superposition of the Stokes component spectra modulating carriers. With proper choice of carrier frequencies, the Stokes components can be isolated in the Fourier domain.

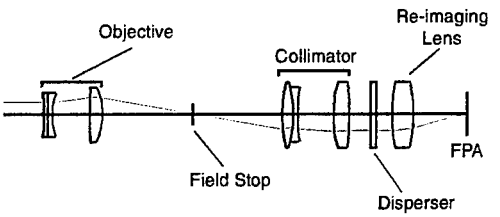

Figure 4: The CTIS Layout. The lens depictions are meant only to be representative of the role each lens plays in the system. Commercial objectives are usually used in the roles of objective, collimator, and re-imaging lens.

frequencies (i.e. proper choice of retarder thicknesses) the Stokes component spectra can be separated in the Fourier domain. This technique is analogous to sideband modulation in radio communications.

The term *channel*, as used in the name given to this technique, occurs as the convergence of two different meanings. In the sideband modulation analogy, individual spectra may be regarded as channels (in analogy to television channels). Dark bands or nulls in an optical spectrum are also termed channels, and a spectrum containing them is sometimes referred to as a channeled spectrum.[6] The carrier waves in the channeled spectropolarimeter result in channeled spectra, as illustrated in Figure 3.

1.2 Computed tomography imaging spectrometry

If used in combination with a snapshot imaging spectrometer, the channeled spectropolarimetry technique acquires snapshot imaging capability. The computed tomography imaging spectrometer (CTIS) is just such a spectrometer. CTIS obtains spatial and spectral data simultaneously by imaging through a computer-generated holographic disperser and carrying out a reconstruction using the mathematics of limited-angle tomography.

The basic layout of the CTIS architecture is shown in Figure 4. The objective lens forms an image of the scene under study in the field stop, which defines the instrument's field of view. The light from this image is then collimated, passed through a computer-generated holographic disperser (CGH) and imaged onto a camera's FPA. The image from each wavelength present in the scene is dispersed into a grid of diffraction orders on the FPA, with the separation between orders increasing with wavelength.

Imaging spectrometers gather data over a three-dimensional (x, y, and λ) volume, sometimes referred to as the object cube. The object cube is a subset of the four-dimensional hypercube discussed earlier. The effect of the dispersion of the CGH can be viewed as generating projections from various angles through the object cube onto the FPA, as illustrated in Figure 5. An estimate of the object cube is reconstructed from these projections by computed tomography. The reconstruction is quite computationally intensive and is carried out on a high-performance computer workstation. The spatial and spectral resolution achieved is constrained in part by the number of pixels in the focal plane array. As one would expect, increasing the number of pixels allows finer sampling of the spatial and spectral content of the image and therefore better spatial and spectral resolution. The complete CTICS system is obtained by combining the channeled spectropolarimeter and CTIS systems, as illustrated in Figure 6. Prototypes are under development for the visible and short wave infrared portions of the spectrum. The design examples given here apply to the system for the visible spectrum.

2 RETARDER DESIGN

Assuming each retarder is fashioned from a single crystalline material, cut with its optic axis parallel to the retarder's faces, then each retardance δ_k will follow

$$\delta_k = 2\pi d_k \Delta n_k \sigma. \tag{1}$$

The retarder's thickness is given by d_k and Δn_k is its birefringence (the difference in indices of refraction for its slow and fast axes). It is clear from Equation 1 that the retardance of each retarder will vary nominally in proportion to

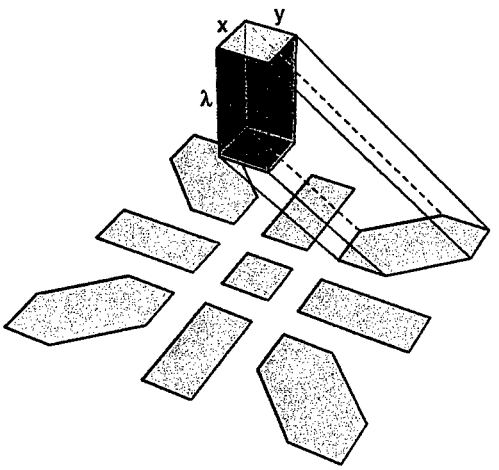

Figure 5: The dispersion of the CGH causes the separation of diffraction orders to increase with wavelength, resulting in several projections of the object cube onto the FPA.

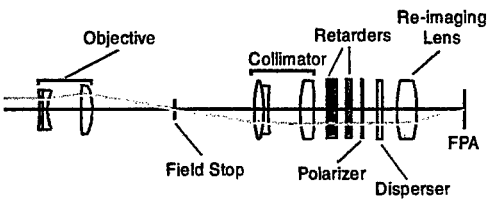

Figure 6: The CTICS Layout. The lens depictions are meant only to be representative of the role each lens plays in the system. Commercial objectives are usually used in the roles of objective, collimator, and re-imaging lens.

wavenumber σ. This dependence on wavenumber gives rise to the carrier waves in the sideband modulation analogy via factors of $\cos\delta_k$ and $\sin\delta_k$ which arise in a treatment of the system using the Mueller calculus. (See Sabatke *et al.*[7] for further details.)

The frequency of these sinusoids is set by the product of the retarder's thickness and birefringence, which may be recognized as the optical path difference (OPD) between the paths of rays polarized respectively along the slow and fast axes of the retarder. In many polarization applications, retarders are made as thin as possible in order to minimize the variation of retardance with wavelength. In the channeled spectropolarimeter, by contrast, the OPDs are deliberately designed with substantial values (which is why the retarders are referred to as *thick*). In real systems, the proportionality between retardance and wavenumber is imperfect because of dispersion in the material from which the retarder is fabricated. That is, the birefringence Δn_k in general depends on σ.

Some care is necessary in using the terminology of spectral analysis, since it can be applied in several ways to the channeled spectropolarimeter. Terms such as *frequency*, *band*, and *band-limited* apply to functions both of wavenumber σ and its conjugate variable under the Fourier transform, which we will denote s. In order to distinguish between the two meanings, we will often prepend σ or s to these terms.

Our system for the visible spectrum will operate over a wavelength range of 0.4–0.7 μm or a wavenumber range of 1.4–2.5 μm^{-1}. Our goal is to resolve 16 samples across the spectrum for each Stokes component spectrum. A 25% margin of extra s-bandwidth is designed into the system by using a value of 20 in place of 16. Then the OPD of the first retarder is calculated as

$$d_1\Delta n_1 \approx \frac{20}{1.1\,\mu\text{m}^{-1}} \approx 18\,\mu\text{m}. \tag{2}$$

In order to obtain equally spaced channels (as illustrated in Figure 3) the retarders should have a 1:2 ratio in OPD. Thus the second retarder should have an OPD of about 36 μm. Dividing by the birefringence $\Delta n \approx 0.0096$ for quartz yields correspondng thicknesses of 1.9 mm and 3.8 mm respectively.

The tolerances on the thicknesses are fairly relaxed, since we are interested in setting the modulation frequency and not a specific number of waves of retardance. Tolerances of $\pm 0.5\%$ were specified to the vendor. The flatness of the retarder faces was specified at a quarter wave (at a test wavelength of 0.633 μm). It is possible for the thickness of the retarder to vary across its aperture as a result of a wedge angle between the faces. The result of such variation is that the carrier waves consist of a superposition of many sinusoids with slightly different frequencies. With increasing σ these sinusoids fall out of phase and begin to interfere destructively, resulting in a reduction of the carrier frequency amplitude.

For back-of-the-envelope purposes, we may assume that the frequencies which result from thickness variations in the retarder are uniformly distributed in a range Δh about a nominal carrier frequency h_{nom}. The carrier wave can then be represented as

$$\int \frac{1}{\Delta h}\,\text{rect}\left(\frac{h - h_{\text{nom}}}{\Delta h}\right) e^{i2\pi h\sigma}\,\text{d}h = \text{sinc}(\Delta h\,\sigma)\,e^{i2\pi h_{\text{nom}}\sigma}. \tag{3}$$

Thus the carrier takes the form of a sinusoid at the nominal frequency h_{nom} with its amplitude modified by a sinc envelope. As shown in Figure 7, the envelope tends to fall with increasing σ. Then if we dictate that the carrier amplitude must not drop below a specified amount (indicated by the dashed line in the figure), the value of the envelope at the upper wavenumber limit of the system's spectral band will be the key consideration. For example, to just meet a 95% amplitude requirement (that is, to have $\text{sinc}(\Delta h\,2.5\,\mu\text{m}^{-1}) \approx 0.95$), a value of $\Delta h \approx 0.070\,\mu$m is required. This corresponds to a variation of 7.3 μm in thickness across the retarder's face. For a 1 inch diameter element, we arrive at a wedge tolerance of 60 seconds of arc. A margin of safety is allowed by specifying a tolerance of 15 seconds of arc. The retarders were fabricated with 1 inch diameter and a broad band anti-reflection coating on each face.

2.1 Non-imaging prototype

A non-imaging channeled spectropolarimeter has been assembled for demonstration of the method and development of calibration and data processing techniques. Retarders with a 3:1 ratio in OPD (rather than 1:2) are used. This is primarily a legacy of early treatments of channeled spectropolarimetry. The 1:2 ratio makes more efficient use of

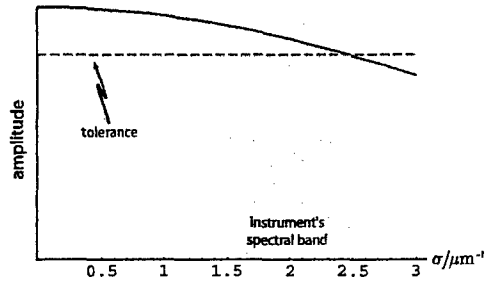

Figure 7: Variations in retarder thickness result in a roll-off of carrier amplitude across the spectrum.

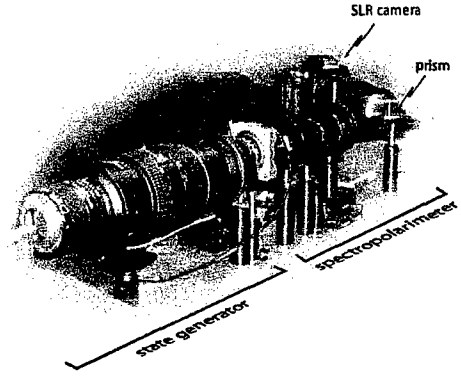

Figure 8: Experimental set-up for the visual demonstration of the channeled spectropolarimeter.

s-bandwidth in the spectrometer, and will likely be preferred for most purposes. However the principles of operation are the same for both configurations.

For quantitative measurements the beam exiting the analyzer is coupled into an optical fiber, and a fiber spectrometer is employed as the detector. A striking visual demonstration can be performed by replacing the fiber and spectrometer with a prism and SLR camera, allowing inspection of the channeled spectra with one's own eyes in the camera viewfinder. Figure 8 shows the system. A spectral polarization state generator, consisting of a white light beam sent through a polarizer and achromatic quarter wave plate, is used to control the input polarization state. Figure 9 shows spectra obtained with a similar setup (which differs in the use of a cylindrical lens to broaden the spectra in the direction perpendicular to that of the dispersion, and in the use of a digital camera to record the images).

3 CTIS DESIGN

The resolution required of the spectrometer is related to the desired resolution of the Stokes component spectra by a factor of seven (as can be seen by counting the s-domain channels in Figure 3). Since we are designing for 20 resolution bands in each channel, we require 140 resolution bands in the CTIS, giving

$$\delta\sigma_{\mathrm{CTIS}} \approx \frac{1.1\,\mu\mathrm{m}^{-1}}{140} \approx 7.9 \times 10^{-3}\,\mu\mathrm{m}^{-1}. \tag{4}$$

The resolution of the CTIS is a complicated topic. The tomographic imaging method, calibration techniques and reconstruction techniques are all likely to impact its resolution. Practical estimates may be taken from the number of different wavelengths at which the system is calibrated and the number of FPA array pixels spanned by the CGH diffraction orders. Because CTIS is a grating spectrometer, any attempt to characterize its spectral resolution as a

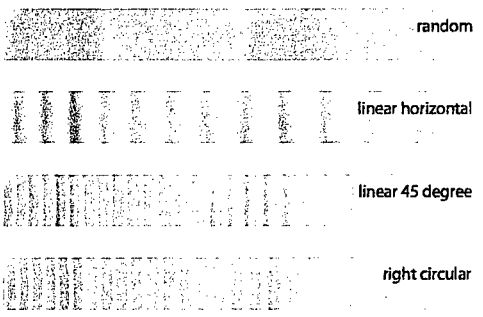

Figure 9: Reverse contrast images of channeled spectra for several different input polarization states, recorded with a system similar to that shown in Figure 8.

single value should probably be made in terms of wavelength rather than wavenumber. Wavelength resolution $\delta\lambda$ and wavenumber resolution $\delta\sigma$ are related (taking both to be positive) by

$$\delta\lambda = \frac{\delta\sigma}{\sigma^2}. \tag{5}$$

Assuming the CTIS wavelength resolution to be constant across the spectrum, its required value can be conservatively estimated by using the largest value acquired by the wavenumber in Equation 5. This yields $\delta\lambda \approx 1.3\,\text{nm}$, which corresponds to about 240 resolution bands in the CTIS. With this arrangement, the CTIS meets the wavenumber resolution requirement at the blue end of the spectrum and exceeds it (that is $\delta\sigma$ is smaller than necessary) toward the red.

In order to achieve 240 bands of resolution, the highest diffraction order in the CTIS (with a white input) should span at least as many pixels on the FPA. Table 1 gives the prescription for a CTIS system we have designed which meets this requirement. The prescription features a 2048×2048 pixel FPA (as shown in the left column of the table), collimating and reimaging optics with respective focal lengths of 300 mm and 60 mm, a 2 mm square field stop, and a period in the CGH of 16 μm (as shown in the right column). The system is intended to make use of a 5×5 array of diffraction orders (including the 0, ±1, and ±2 orders). The figure in Table 1 shows the footprint of the field stop after diffraction for each of the orders. The highest order is diffracted across more than 300 pixels, which meets our goal for spectral resolution. The direct (zero order) image of the field stop measures on the order of 50 pixels on a side. Hence we anticipate approximately 50×50 elements of spatial resolution and 16 elements of spectral resolution in each of the four Stokes components in the final CTICS system.

The CTIS prescription in Table 1 specifies the required period of the CGH. There is however considerable additional effort required to design a suitable CGH.[8] The CGH designer's task is to tailor the diffraction efficiencies of the orders so they increase modestly with order number in those orders used by the system (in this case the 0, ±1, and ±2 orders in both FPA dimensions), fall off sharply at higher order numbers to avoid sending light into unused orders, and remain well-behaved across a broad wavelength band. A phase-only hologram is used to preserve throughput.

The hologram is formed by etching a prescribed surface relief pattern into the face of a transparent substrate. The pattern is periodic, and is formed by replicating a smaller pattern (the unit cell) over the grating's face. The surface relief of the unit cell is described on a rectangular grid, with surface height taken to be constant within each grid element. Each element of the unit cell is termed a phase element (or *phasel*). For this instrument, the CGH unit cell was chosen to consist of an 8 × 8 array of phasels. Table 2 shows design data and the surface relief of the disperser designed for the spectropolarimeter. It was fabricated in PMMA using an electron beam etch.

Initial assembly of the CTICS has been carried out. Figure 10 shows a raw focal plane image. The object is a diagonal line in the field stop composed of white horizontal linearly polarized light.

Table 1: Prescription for the CTIS portion of the imaging channeled spectropolarimeter.

optical prescription	
field stop size / mm	CGH period / μm
2.00	16.00
collimator efl / mm	reimaging efl / mm
300	60
CGH aperture / mm	
19.0	

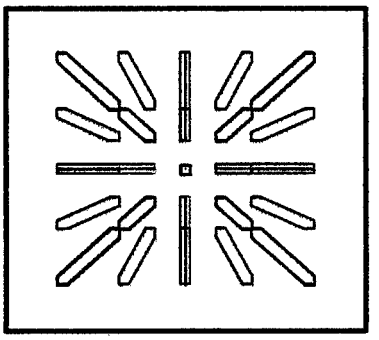

Focal Plane Array size	
x pixels	y pixels
2048	2048
x pixel size / μm	y pixel size / μm
7.4	7.4

wavelength range / μm	
low	high
0.4	0.7

Table 2: Design data for the holographic grating. The image is a computer's rendition of a 2 × 2 array of unit cells on the disperser's face.

material:	PMMA
index of refraction:	1.49608
maximum PV phase depth:	1.65*2π
design wavelength:	0.51 μm
performance band:	0.4-0.7 μm
Grating period:	16 μm
pixels per cell:	8x8
pixel size:	2 μm x 2 μm
distribution:	analog depth
full area:	19 mm active area on a 1" substrate

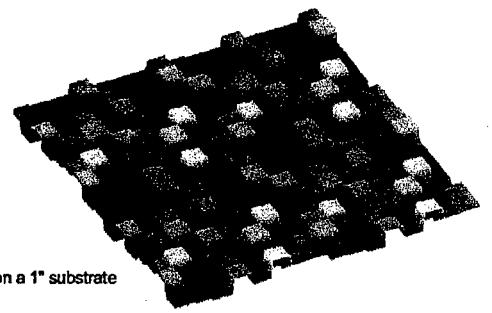

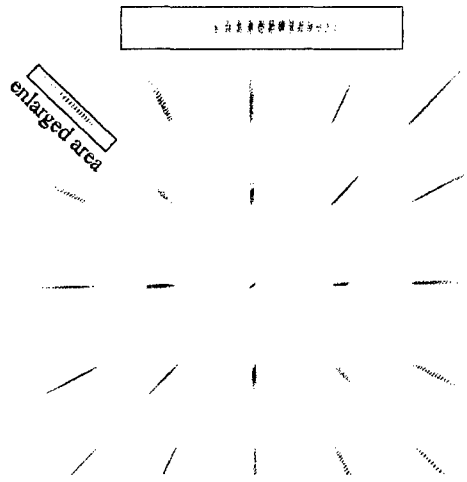

Figure 10: Reverse contrast raw image obtained at the focal plane of a CTICS system. The object is a diagonal line of white, horizontal linearly polarized light. A high diffraction order is shown magnified.

4 CONCLUSIONS

With the addition of a few polarization elements to the CTIS architecture, the spectral dependence of all four Stokes vector components is encoded in the measured spectrum. This synthesis of computed tomography imaging spectrometry and channeled spectropolarimetry holds great promise for a new imaging spectropolarimeter, CTICS. With a single focal plane array and snapshot capability, CTICS offers a novel solution to the limitations of conventional spectrometers and polarimeters. It is particularly well suited to the demands of rapidly changing scenes, as encountered in the identification and tracking of moving targets. We have discussed design considerations for CTICS instruments and are developing prototypes for the visible and short wave infrared. Ongoing work also includes development of calibration and data reconstruction techniques.

REFERENCES

[1] G. Forrsell, "Surface landmine and trip-wire detection using calibrated polarization measurements in the LWIR and SWIR," in *Subsurface and Surface Sensing Technologies and Applications III*, pp. 41–51, 2001.

[2] K. Oka and T. Kato, "Spectroscopic polarimetry with a channeled spectrum," *Opt. Lett.*, vol. 24, no. 21, pp. 1475–7, 1999.

[3] F. J. Iannarilli, S. H. Jones, H. E. Scott, and P. Kebabian, "Polarimetric-spectral intensity modulation (P-SIM): enabling simultaneous hyperspectral and polarimetric imaging," in *Infrared technology and applications XXV*, pp. 474–81, 1999.

[4] F. J. Iannarilli, J. A. Shaw, S. H. Jones, and H. E. Scott, "Snapshot LWIR hyperspectral polarimetric imager for ocean surface sensing," in *Polarization Analysis, Measurement, and Remote sensing III*, pp. 270–83, 2000.

[5] M. R. Descour, C. E. Volin, E. L. Dereniak, K. J. Thome, A. B. Schumacher, D. W. Wilson, and P. D. Maker, "Demonstration of a high-speed nonscanning imaging spectrometer," *Opt. Lett.*, vol. 22, no. 16, pp. 1271–3, 1997.

[6] R. W. Ditchburn, *Light.* London: Academic, 3 ed., 1976.

[7] D. Sabatke, A. Locke, E. L. Dereniak, M. Descour, J. Garcia, T. Hamilton, and R. W. McMillan, "Snapshot imaging spectropolarimeter," *Opt. Eng.*, vol. 41, no. 5, pp. 1048–1054, 2002.

[8] C. E. Volin, *Portable snapshot infrared imaging spectrometer.* PhD thesis, University of Arizona, Tucson, Arizona, 2000.